

ORIGINAL PAPER

Open Access



Effects of systemic ventricular assist in failing Fontan patients: a theoretical analysis using a computational model

Eiri Kisamori¹, Yasuhiro Kotani^{1*}, Toshiaki Shishido², Shingo Kasahara¹ and Shuji Shimizu^{1,2*} 

Abstract

Mechanical circulatory support is a potential treatment for failing Fontan patients. In this study, we performed a theoretical analysis using a computational model to clarify the effects of systemic ventricular assist device (VAD) in failing Fontan patients. Cardiac chambers and vascular systems were described using the time-varying elastance model and modified Windkessel model, respectively. A VAD was simulated as a nonlinear function. In systolic and diastolic ventricular dysfunction and atrioventricular valve regurgitation models, systemic VAD increased the cardiac index and decreased the central venous pressure (CVP). However, in the high pulmonary vascular resistance model, CVP became extremely high above 15 mmHg to maintain the cardiac index when the pulmonary vascular resistance index (PVRI) was above 5 Wood units m². In Fontan patients with ventricular dysfunction or atrioventricular valve regurgitation, systemic VAD efficiently improves the hemodynamics. In Fontan patients with PVRI of > 5 Wood units m², systemic VAD seems ineffective.

Keywords Ventricular assist device, Failing Fontan, Hemodynamic simulation, Lumped parameter model

Introduction

Since the Fontan palliation was introduced in 1968 [1], the Fontan procedure has been the goal of surgical palliation in patients with a functional single ventricle. Despite remarkable improvements in early survival [2], their quality of life and life expectancy after Fontan procedure are unsatisfactory because of the multiple organ system dysfunction that often occurs in the long term [3]. Fontan circulation may collapse

due to various reasons, such as systolic and/or diastolic ventricular dysfunction, atrioventricular valve regurgitation and the elevation of pulmonary vascular resistance [4, 5]. In the acutely failing Fontan circulation, mechanical circulatory support is required, but it has still been a challenging issue in Fontan patients. Although several case reports demonstrated success with a right ventricular assist device (VAD) [6], the right ventricular support can be anatomically difficult because the need to disconnect the cavopulmonary connection to insert a VAD [7]. On the other hand, the introduction of systemic (left-sided) ventricular assist is technically easier even in the Fontan patients. However, the appropriate situation for the systemic ventricular assist in the Fontan circulation has remains controversial.

There have been several simulation studies focusing on the Fontan circulation. However, previous computational simulation studies of VAD in the Fontan circulation have

*Correspondence:

Yasuhiro Kotani
yasuhiro.kotani@cc.okayama-u.ac.jp
Shuji Shimizu
shujismz@ncvc.go.jp

¹ Department of Cardiovascular Surgery, Okayama University Graduate School of Medicine, Dentistry, and Pharmaceutical Sciences and Okayama University Hospital, 2-5-1 Shikatacho, Kitaku, Okayama 700-8558, Japan

² Department of Research Promotion and Management, National Cerebral and Cardiovascular Center, 6-1 Kishibe-Shimmachi, Suita, Osaka 564-8565, Japan



© The Author(s) 2024. **Open Access** This article is licensed under a Creative Commons Attribution 4.0 International License, which permits use, sharing, adaptation, distribution and reproduction in any medium or format, as long as you give appropriate credit to the original author(s) and the source, provide a link to the Creative Commons licence, and indicate if changes were made. The images or other third party material in this article are included in the article's Creative Commons licence, unless indicated otherwise in a credit line to the material. If material is not included in the article's Creative Commons licence and your intended use is not permitted by statutory regulation or exceeds the permitted use, you will need to obtain permission directly from the copyright holder. To view a copy of this licence, visit <http://creativecommons.org/licenses/by/4.0/>.

mainly focused on the modes and patterns of VAD. Pekkan et al. tested four different pumps and three anatomical pathologies of the total cavopulmonary connection [8]. De Molfetta analyzed the effects of continuous and pulsatile flow VAD on Fontan patients [9]. They also tested the effects of the left and right ventricular and bi-ventricular assist devices in the Fontan circulation [10].

On the other hand, there are little studies focusing on patients' pathophysiology. Therefore, in this study, we perform a computational simulation using a lumped parameter model to clarify which patients are acceptable for systemic ventricular assist therapy alone.

Materials and methods

The electrical analog used to simulate the cardiovascular system of the Fontan circulation with a systemic VAD is shown in Fig. 1. Details of the simulation model have been described previously [11–14]. In this study, an adult man with a body surface area of 1.9 m² was simulated.

Heart

The ventricular and atrial chambers are represented by a time-varying elastance model [11–14]. The pressure and volume of each chamber are related by

$$P_{cc}(t) = [P_{es,cc}(V_{cc}) - P_{ed,cc}(V_{cc})]e_{cc}(t) + P_{ed,cc}(V_{cc}), \quad (1)$$

$$P_{ed,cc} = A_{cc} \left[e^{B_{cc}(V_{ed,cc} - V_{0,cc})} - 1 \right], \quad (2)$$

$$P_{es,cc} = E_{es,cc} [V_{es,cc} - V_{0,cc}], \quad (3)$$

$$e_{cc}(t) = \begin{cases} 0.5[1 - \cos(\pi t/T_{es,cc})] & 0 \leq t < 2T_{es,cc} \\ 0 & 2T_{es,cc} \leq t < T_c \end{cases}, \quad (4)$$

where P_{cc} and V_{cc} are the chamber pressure and volume, respectively [cc denotes single atrial (SA) or single ventricular (SV) chamber], and t is the time from the start of systole. The chamber pressure is modeled as the sum of the end-diastolic pressure ($P_{ed,cc}$ Eq. 2) and developed pressure [difference between end-systolic pressure ($P_{es,cc}$ Eq. 3) and $P_{ed,cc}$] scaled by the normalized elastance [$e_{cc}(t)$, Eq. 4]. The baseline parameters used in this model are listed in Table 1. Each valve was represented as an ideal diode connected serially to a small resistor (R_{AV} , aortic; R_{AVV} , atrioventricular). For patients with atrioventricular valve regurgitation, regurgitation is modeled as a reverse-connected resistor (R_{AVVR}) and diode (see Fig. 1).

Vascular system

Pulmonary and systemic vascular systems were modeled as modified three-element Windkessel models (Fig. 1). Each vascular system is modeled by lumped venous (C_v) and arterial (C_a) capacitances, characteristic impedance (R_c), arterial resistance (R_a), and resistance proximal to C_v (R_v). For each variable, the pulmonary circulation is denoted by adding the subscript (_p, such as $R_{a,p}$), and the systemic circulation is denoted by adding the subscript (_s, such as $R_{a,s}$). The linear relationship between the pressure drops (ΔP) and flows (Q) in each resistance (R) (Eq. 5), the relationship between the pressure (P_c) and volume (V_c) in each capacitance C (Eq. 6), and the change in volume in each capacitance [$dV(t)/dt$] calculated by the difference between the inflow (Q_{inflow}) and outflow ($Q_{outflow}$) (Eq. 7) was used to describe each vascular system:

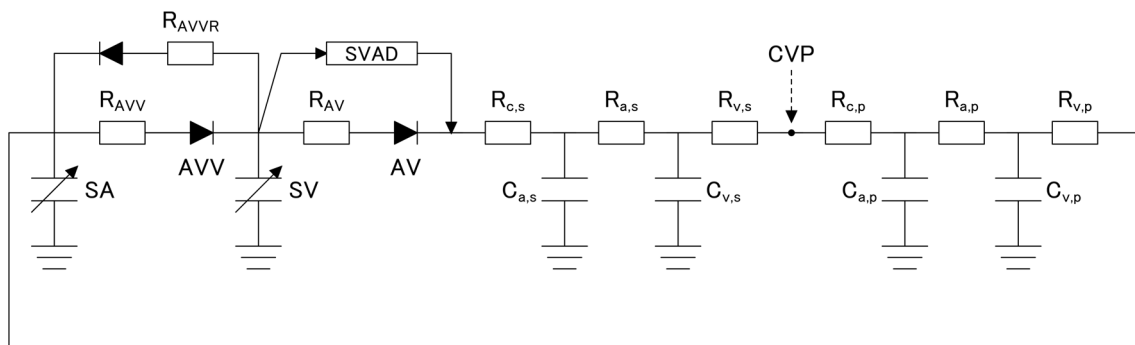


Fig. 1 Lumped parameter model of the Fontan circulation with systemic ventricular assist device. SA single atrium, SV single ventricle, AVV atrioventricular valve, AV aortic valve, SVAD systemic ventricular assist device, CVP central venous pressure. R_{AVV} , R_{AVVR} and R_{AV} donate resistances of atrioventricular valve, atrioventricular valve regurgitation and aortic valve, respectively. $R_{c,s}$ and $R_{c,p}$ donate characteristic impedances of systemic and pulmonary circulation, respectively. $R_{a,s}$ and $R_{a,p}$ donate systemic and pulmonary arterial resistance, respectively. $R_{v,s}$ and $R_{v,p}$ donate systemic and pulmonary venous resistances, respectively. $C_{a,s}$ and $C_{a,p}$ donate systemic and pulmonary arterial capacitances, respectively. $C_{v,s}$ and $C_{v,p}$ donate systemic and pulmonary venous capacitances, respectively

Table 1 Parameter used in the Fontan circulation and ventricular assist device models

Heart rate, beats/min	75	
Duration of cardiac cycle (T_c), ms	800	
Time advance of atrial systole, ms	16	
	SV	SA
Time to end systole ($T_{es,cc}$), ms	200	120
End-systolic elastance ($E_{es,cc}$), mmHg/mL	3	0.5
Scaling factor of EDPVR (A_{cc}), mmHg	0.35	0.06
Exponent for EDPVR (B_{cc}), mL ⁻¹	0.033	0.264
Unstressed volume ($V_{0,cc}$), mL	0	5
Aortic valvular resistance (forward) (R_{AV}), mmHg s mL ⁻¹	0.001	
Atrioventricular valvular resistance (forward) (R_{AVV}), mmHg s mL ⁻¹	0.001	
	Systemic (_s) ^a	Pulmonary (_p) ^b
Arterial resistance (R_a), mmHg s mL ⁻¹	0.7	0.03
Characteristic impedance (R_c), mmHg s mL ⁻¹	0.03	0.02
Venous resistance (R_v), mmHg s mL ⁻¹	0.015	0.015
Arterial capacitance (C_a), mL/mmHg	1.32	13
Venous capacitance (C_v), mL/mmHg	70	8
K_A , mmHg/rpm ²	3.45×10^{-6}	
K_B , mmHg L/min/rpm	-5.9×10^{-5}	
K_C , mmHg L ² /rpm ²	-1.45	

cc denotes single ventricular (SV) or single atrial (SA) chamber. EDPVR, endo-diastolic pressure–volume relation

^a For each variable, the systemic circulation is denoted by adding the subscript (_s, such as $R_{a,s}$)

^b For each variable, the pulmonary circulation is denoted by adding the subscript (_p, such as $R_{a,p}$)

$$\Delta P = QR, \quad (5)$$

$$P_c = \frac{V_c}{C}, \quad (6)$$

$$\frac{dV(t)}{dt} = \sum Q_{inflow}(t) - \sum Q_{outflow}(t), \quad (7)$$

where $Q_{inflow}(t)$ and $Q_{outflow}(t)$ are volumetric inflow and outflow, respectively.

Total stressed blood volume

The total stressed blood volume (V_s) is defined as the sum of the stressed volumes in all capacitances and chambers:

$$V_s = V_{SA} + V_{SV} + V_{C_{a,s}} + V_{C_{v,s}} + V_{C_{a,p}} + V_{C_{v,p}}. \quad (8)$$

Rotational pump model

The flow of a rotational pump was described as a function of the pressure head (ΔP) and rotational frequency (r) in a previous study [15]. Therefore, in this study, a nonlinear function was used to simulate the flow of the rotational pump (Q_{pump}):

$$\Delta P = K_A \cdot r^2 + K_B \cdot r \cdot Q_{pump} + K_C \cdot (Q_{pump})^2. \quad (9)$$

This flow characteristics is similar to that of HeartMate III (Abbott, Abbott Park, IL, USA) (Fig. 2) [16].

Simultaneous differential equations (Eqs. 1–9) were solved using MATLAB/Simulink R2022a (MathWorks, Natick, MA, USA).

Protocols

The effect of systemic VAD in a variety of pathophysiology

First, four types of failing Fontan circulation models—systolic ventricular dysfunction, diastolic ventricular dysfunction, atrioventricular valve regurgitation, and high pulmonary vascular resistance model—were simulated. Because mild elevations in pulmonary vascular resistance index (PVRI) coupled with low cardiac index identify patients at high risk of Fontan failure [17], the PVRI was set at 3 Wood units·m² [$R_{a,p}=0.06$; $R_{v,p}=0.015$; $R_{c,p}=0.02$ (mmHg s mL⁻¹)] except for the high pulmonary vascular resistance model. Because Fahnhorst et al. reported that median central venous pressure before VAD placement was 20 mmHg (IQR, 17.75–22.25 mmHg) [18], the parameters of each model were adjusted to simulate failing Fontan circulation with a cardiac index of 1.9 L/min/m² and a central venous pressure

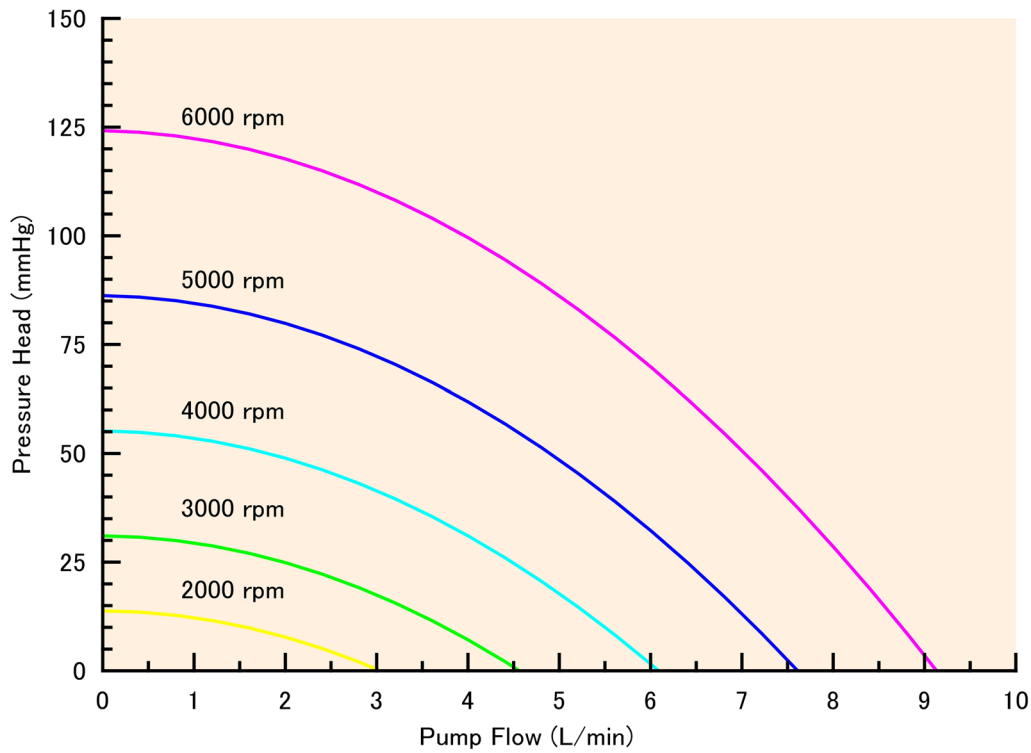


Fig. 2 Non-linear relation between pump flow and pressure head at 2000, 3000, 4000, 5000 and 6000 rpm. This flow-pressure relation is almost similar to that of HeartMate III (Abbott)

of 20 mmHg. Central venous pressure (CVP) was defined as a pressure distal to $R_{v,s}$ (Fig. 1) and calculated by the following equation:

$$CVP = \frac{P_{C_{a,p}} \cdot R_{v,s} + P_{C_{v,s}} \cdot R_{c,p}}{R_{v,s} + R_{c,p}},$$

where $P_{C_{v,s}}$ and $P_{C_{a,p}}$ were the pressures in capacitances $C_{v,s}$ and $C_{a,p}$, respectively.

- (1) In the systolic ventricular dysfunction model (Table S1), $E_{es,sv}$ and stressed blood volume were adjusted to 1.215 mmHg/mL and 2036 mL, respectively.
- (2) In the diastolic ventricular dysfunction model (Table S2), B_{sv} and stressed blood volume were adjusted to 0.0511 mL^{-1} and 1999 mL, respectively.
- (3) In the atrioventricular valve regurgitation model (Table S3), R_{AVVR} and stressed blood volume were adjusted to $0.225 \text{ mmHg s mL}^{-1}$ and 2015 mL, respectively.
- (4) In the high pulmonary vascular resistance model (Table S4), $R_{a,p}$ and stressed blood volume were adjusted to be $0.23 \text{ mmHg s mL}^{-1}$ and 1903 mL, respectively.

Second, in each failing Fontan circulation model, systemic VAD was instituted from the single ventricle to the aorta, and the rotational frequency was increased from 3000 to 4000 rpm. At a rotational frequency of 4000 rpm, the stressed blood volume was drawn stepwise in decrements of 100 mL until the mean pressure or volume of each chamber reached approximately zero, but not the minimum pressure or volume below zero. If the pressure or volume of each chamber reached below zero after VAD initiation, the stressed blood volume was increased stepwise in increments of 100 mL until the pressure or volume reached above zero. When the stressed blood volume was varied, the initial volume for systemic venous capacitance was decreased or increased and the simulation was started. After several dozen beats of simulation, the steady-state hemodynamic values were collected.

Effect of pulmonary vascular resistance on systemic VAD

$R_{a,p}$ was increased stepwise from 0.06 to $0.25 \text{ mmHg s mL}^{-1}$ (PVRI: 3 to 9 Wood units $\cdot \text{m}^2$) in a systolic and diastolic ventricular dysfunction model ($E_{es,sv} = 1.215 \text{ mmHg/mL}$, $B_{sv} = 0.0511 \text{ mL}^{-1}$) under systemic ventricular assist at a rotational frequency of 3500 rpm to evaluate the effect of elevated pulmonary vascular resistance. The stressed blood volume was

controlled to achieve a mean pressure of approximately 0 mm Hg for a single atrium. Cardiac index, mean single atrial pressure, mean central venous pressure, and mean blood pressure were calculated for each PVRI.

Results

When a systolic ventricular dysfunction model with $E_{es,sv}$ of 1.215 mmHg/mL and stressed blood volume of 2036 mL was simulated, a cardiac index of 1.91 L/min/m² and a systemic central venous pressure of 20.0 mmHg were achieved (Table 2.). Once the systemic VAD was initiated at a rotational frequency of 3000 rpm, the cardiac index increased to 2.89 L/min/m². Central venous pressure was maintained at 19.7 mmHg. After increasing the rotational frequency to 4000 rpm, the cardiac index was

3.23 L/min/m², and central venous pressure was maintained at 19.6 mmHg with single atrial and mean blood pressures of 9.92 mmHg and 95.7 mmHg, respectively (Fig. 3). When the stressed blood volume was reduced to 1136 mL (minus 900 mL), the single atrial pressure reached 1.18 mmHg, cardiac index was 3.20 L/min/m², mean blood pressure was 86.4 mmHg, and central venous pressure was 10.8 mmHg (Fig. 3).

When a diastolic ventricular dysfunction model with B_{sv} of 0.0511 mL⁻¹ and stressed volume of 1999 mL was simulated, cardiac index was 1.90 L/min/m² and systemic central venous pressure was 20.0 mmHg (Table 2.). Once the systemic VAD was initiated at a rotational frequency of 3000 rpm, the cardiac index increased to 3.13 L/min/m² and central venous pressure was maintained

Table 2. Effect of systemic ventricular assist device in a variety of pathophysiology

<i>Systolic ventricular dysfunction</i>					
End-systolic elastance ($E_{es,sv}$), mmHg/mL	1.215				
Stressed blood volume, mL	2036	2036	2036	2036	1136
Cardiac index, L/min/m ²	1.91	2.89	3.05	3.23	3.20
Mean blood pressure, mmHg	65.0	87.8	91.7	95.7	86.4
Central venous pressure, mmHg	20.0	19.7	19.7	19.6	10.8
Single atrial pressure, mmHg	14.3	11.0	10.5	9.92	1.18
Rotational frequency, rpm		3000	3500	4000	4000
<i>Diastolic ventricular dysfunction</i>					
Exponent for EDPVR (B_{sv}), mL ⁻¹	0.0511				
Stressed blood volume, mL	1999	1999	1999	1999	1199
Cardiac index, L/min/m ²	1.90	3.13	3.33	3.53	3.20
Mean arterial blood pressure, mmHg	65.0	93.5	98.1	102.7	87.1
Central venous pressure, mmHg	20.0	19.7	19.6	19.5	11.5
Single atrial pressure, mmHg	14.3	10.2	9.58	8.93	1.82
Rotational frequency, rpm		3000	3500	4000	4000
<i>Atrioventricular valve regurgitation</i>					
Regurgitation resistance (R_{AVR}), mmHg s mL ⁻¹	0.225				
Stressed blood volume, mL	2015	2015	2015	2015	1115
Cardiac index, L/min/m ²	1.90	3.00	3.18	3.37	3.20
Mean arterial blood pressure, mmHg	65.0	90.4	94.8	99.2	86.3
Central venous pressure, mmHg	20.0	19.7	19.7	19.6	10.6
Single atrial pressure, mmHg	14.3	10.7	10.1	9.51	1.00
Regurgitation fraction, %	50.9	41.1	39.6	38.0	2.00
Rotational frequency, rpm		3000	3500	4000	4000
<i>High pulmonary vascular resistance</i>					
Pulmonary arterial resistance (R_{ap}), mmHg s mL ⁻¹	0.230				
Stressed blood volume, mL	1903	1903	2203	2503	
Cardiac index, L/min/m ²	1.91	2.40	2.80	3.20	
Mean arterial blood pressure, mmHg	65.0	77.4	90.1	102.9	
Systemic central venous pressure, mmHg	20.0	20.7	24.0	27.3	
Single atrial pressure, mmHg	4.01	0.506	0.445	0.382	
Rotational frequency, rpm		3000	3500	4000	

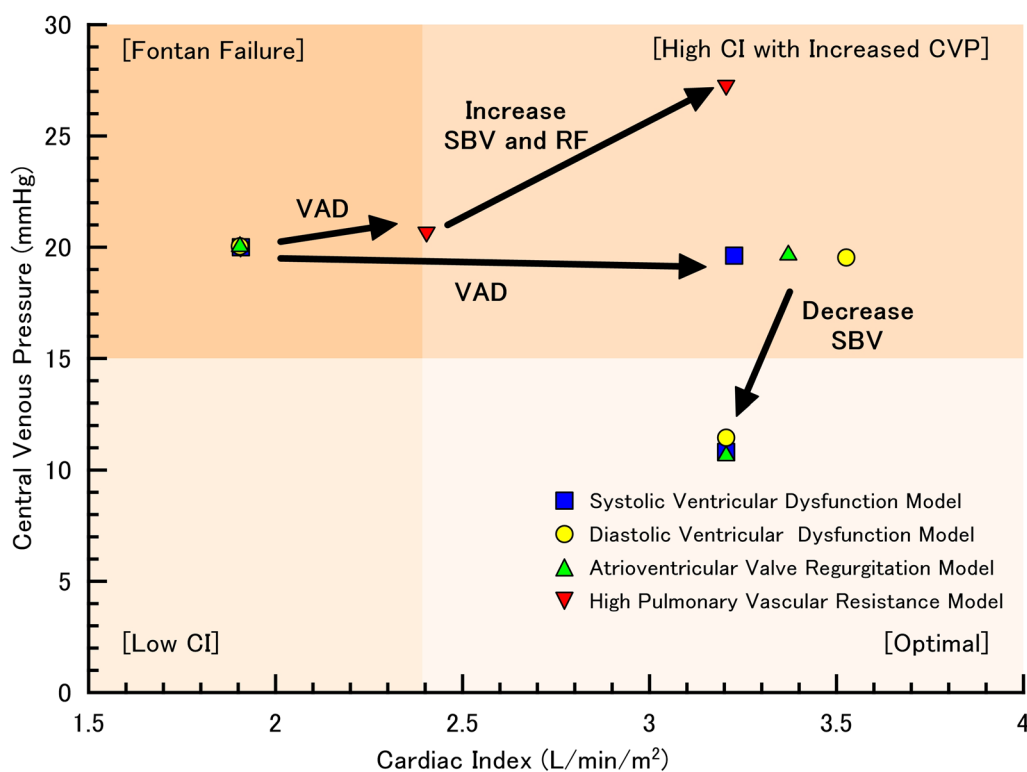


Fig. 3 Ration between cardiac index and central venous pressure before and after ventricular assist. First, ventricular assist device (VAD) was introduced without altering stressed blood volume (SBV). The rotational frequency (RF) of VAD was set at 4000 rpm in systolic and diastolic dysfunction models and atrioventricular valve regurgitation model and at 3000 rpm in high pulmonary vascular resistance model. Next, The RF of VAD was set at 4000 rpm and then the SBV was adjusted in increments or decrements of 100 mL to become the mean single atrial pressure around zero, but not the minimum pressure below zero. Blue squares and yellow circles represent the simulation results in systolic and diastolic dysfunction models, respectively. Light-green triangles represent those in atrioventricular valve regurgitation model. Red inverted triangles represent those in high pulmonary vascular resistance model

at 19.7 mmHg. After increasing the rotational frequency to 4000 rpm, the cardiac index was 3.53 L/min/m² and central venous pressure remained at 19.5 mmHg (Fig. 3). The single atrial and mean blood pressures were 8.93 mmHg and 102.7 mmHg, respectively. When the stressed blood volume was reduced to 1199 mL (minus 900 mL) in this model, the single atrial pressure reached 1.82 mmHg. The cardiac index was 3.20 L/min/m², mean blood pressure was 87.1 mmHg, and central venous pressure decreased to 11.5 mmHg (Fig. 3).

When an atrioventricular valve regurgitation model with R_{AVVR} of 0.225 mmHg s mL⁻¹ and stressed blood volume of 2015 mL was simulated, the cardiac index was 1.90 L/min/m², the central venous pressure was 20.0 mmHg, and the regurgitation fraction was 50.9% (Table 3). Once the systemic VAD was initiated at a rotational frequency of 3000 rpm, the cardiac index increased to 3.00 L/min/m², and central venous pressure was maintained at 19.7 mmHg. After increasing the rotational frequency to 4000 rpm, the cardiac index was 3.37 L/min/m², and central venous pressure remained

at 19.6 mmHg with single atrial and mean blood pressures of 9.51 mmHg and 99.2 mmHg, respectively (Fig. 3). When the stressed blood volume was reduced to 1115 mL (minus 900 mL), the single atrial pressure was 1.00 mmHg, cardiac index was 3.20 L/min/m², mean blood pressure was 86.3 mmHg, and central venous pressure was 10.6 mmHg (Fig. 3).

In a high pulmonary vascular resistance model with $R_{a,p}$ of 0.230 mmHg s mL⁻¹ (PVRI = 8.39 Wood units m²) and stressed blood volume of 1903 mL, cardiac index was 1.91 L/min/m² and central venous pressure was 20.0 mmHg (Table 2). Once systemic VAD was initiated at a rotational frequency of 3000 rpm, the cardiac index and central venous pressure increased to 2.40 L/min/m² and 20.7 mmHg, respectively. To increase the rotational frequency above 3000 rpm, an additional stressed blood volume was required in this model. At a rotational frequency of 4000 rpm, an additional stressed blood volume of 600 mL was required to maintain the pressure or volume of each chamber above zero. Then, cardiac index became 3.20 L/min/m², the mean blood pressure

Table 3 Effect of pulmonary vascular resistance in patients with systemic ventricular assist device

Pulmonary vascular resistance index, Woods units m ²	3.01	3.96	5.07	6.02	6.97	8.08	9.03
Pulmonary arterial resistance ($R_{a,p}$), mmHg s mL ⁻¹	0.06	0.09	0.125	0.155	0.185	0.22	0.25
End-systolic elastance ($E_{es,sv}$), mmHg/mL	1.215						
Exponent for EDPVR (β_{sv}), mL ⁻¹	0.0511						
Rotational frequency, rpm	3500						
Stressed blood volume, mL	910	1135	1397	1621	1846	2108	2332
Cardiac index, L/min/m ²	2.80	2.80	2.80	2.80	2.80	2.80	2.80
Mean arterial blood pressure, mmHg	74.9	77.5	80.6	83.3	86.0	89.1	91.7
Central venous pressure, mmHg	8.70	11.4	14.5	17.1	19.8	22.9	25.6
Single atrial pressure, mmHg	0.260	0.263	0.262	0.256	0.260	0.259	0.253

was 102.9 mmHg, and the central venous pressure was increased to 27.3 mmHg (Fig. 3).

Finally, we simulated the model in which pulmonary vascular resistance was varied. With the stepwise increase in $R_{a,p}$, the PVRI increased from 3 to 9 wood units m². Stressed blood volume was controlled to maintain a mean single atrial pressure of approximately 0 mmHg, but not the minimum pressure below 0 mmHg. When the PVRI was 3 Wood units m², the stressed

blood volume was 910 mL. Higher PVRI required larger stressed blood volume to maintain the single atrial pressure above 0 mmHg. An additional stressed blood volume of 1422 mL was required to maintain the single atrial pressure above 0 mmHg when the PVRI was 9 Wood units m² compared with that at a PVRI of 3 Wood units m². A higher PVRI required more stressed blood volume, resulting in a remarkable increase in central venous pressure (Table 3; Fig. 4).

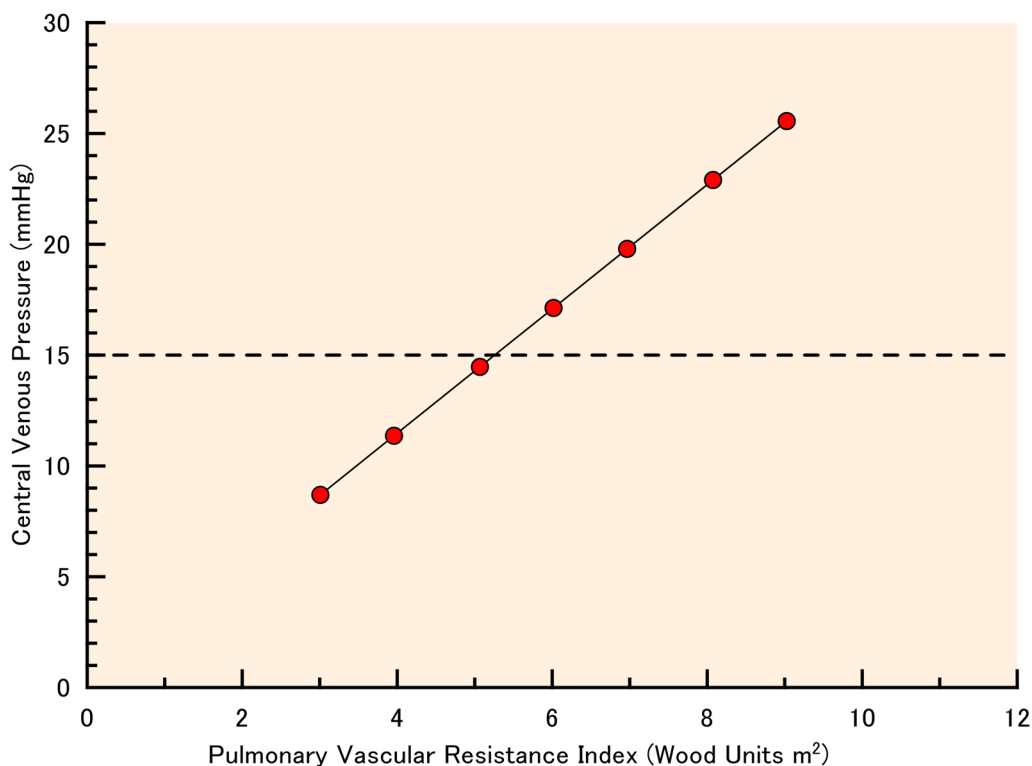


Fig. 4 Relation between pulmonary vascular resistance index and central venous pressure. When pulmonary vascular resistance index (PVRI) was varied from 3 to 9 Wood units m², the rotational frequency of ventricular assist device was set at 3500 rpm and the stressed blood volume was adjusted in increments of 1 mL to become the mean single atrial pressure around zero, but not the minimum pressure below zero. With an increase in PVRI, the central venous pressure rapidly increased. If we define acceptable central venous pressure as less than 15 mmHg, systemic ventricular assist tolerates PVRI less than 5 Wood units m²

Discussion

In this study, four types of failure pathophysiology, systolic and diastolic ventricular dysfunction, atrioventricular valve regurgitation and elevated pulmonary vascular resistance, were simulated to evaluate the efficacy of systemic VAD on the Fontan circulation. This study demonstrated that systemic VADs are effective in patients with systolic and/or diastolic ventricular dysfunction, atrioventricular valve dysfunction, or even with elevated pulmonary vascular resistance when PVRI is less than 5 Wood units·m².

Systolic ventricular dysfunction

In the first few decades after the Fontan procedure, systolic ventricular function is usually preserved but declines over time [19, 20]. Systolic ventricular dysfunction after the Fontan procedure has been reported to be associated with high mortality [21]. Fahnhorst et al. demonstrates the effectiveness of the single VAD in the Fontan patients with systolic ventricular dysfunction [18]. In this study, the initiation of a systemic VAD remarkably increased the cardiac index and blood pressure. At the time of initiating systemic VAD, the decrease in central venous pressure was less than 0.5 mmHg. After reducing stressed blood volume, central venous pressure achieved an acceptable value of 10.8 mmHg in this model. Then, cardiac index and mean blood pressure were maintained at 3.20 L/min/m² and 86.4 mmHg, respectively, and this demonstrates that the cardiac index and blood pressure increased without a decrease in central venous pressure once the systemic VAD was initiated. Stressed blood volume reduction is necessary to decrease central venous pressure while maintaining an adequate cardiac index and mean blood pressure. Therefore, in clinical settings, systemic VAD implantation enables a decrease in central venous pressure by dehydrating patients with the use of diuretics or hemodialysis, as the pathophysiology of this condition is characterized by maintaining cardiac output by increasing the stressed blood volume.

Diastolic ventricular dysfunction

A substantial number of patients with Fontan circulation have diastolic ventricular dysfunction [22, 23]. The use of systemic VADs for diastolic ventricular dysfunction in absence of systolic failure remains controversial. In this study, diastolic ventricular dysfunction model showed a similar trend to the systolic ventricular dysfunction model. The initiation of systemic VAD remarkably increased the cardiac index and blood pressure without decreasing the central venous pressure. After stressed blood volume reduction, central venous pressure dropped with adequate cardiac index (3.20 L/min/

m²) and mean blood pressure (87.1 mmHg). Therefore, reduction of stressed blood volume is possible in Fontan patients with diastolic ventricular dysfunction who have systemic VAD support to achieve a lower central venous pressure.

Atrioventricular valve regurgitation

More than moderate atrioventricular valve regurgitation is a significant risk factor for long-term mortality in Fontan patients [24]. Most patients experience valve failure during the first 30 years of life [25]. Significant atrioventricular regurgitation compromises Fontan circulation due to volume overload, ventricular dilatation, reduced ventricular function, and increased postcapillary and central venous pressures. Although a variety of techniques have been described for valve repair, attaining a competent valve is often challenging, and valve replacement is inevitable in some cases [26, 27]. Cedars et al. reported that 65% of Fontan patients implanted with a VAD had moderate or severe atrioventricular regurgitation [28]. In the atrioventricular valve regurgitation model, systemic VAD is also effective, but a reduction in the stressed blood volume is necessary to achieve an acceptable low central venous pressure. A question may arise whether valve repair is necessary when systemic VAD is established. In fact, Nandi et al. reported a technique for atrioventricular valve excision in continuous-flow ventricular assist device implantation [29]. However, findings of this study suggest that valve repair is unnecessary with the support of a systemic VAD. Therefore, atrioventricular valve regurgitation itself may not impede systemic VAD implantation.

Elevated pulmonary vascular resistance

In the absence of a subpulmonary pump, increased pulmonary vascular resistance is critical, as it causes upstream congestion and decreased downstream flow. In pump failure and valve failure models (systolic ventricular dysfunction, diastolic ventricular dysfunction, and atrioventricular valve regurgitation), this study demonstrated significant hemodynamic improvement under moderately high pulmonary vascular resistance (PVRI=3.01 Wood units·m²). However, systemic VAD did not work well in a remarkably high pulmonary vascular resistance model with an $R_{a,p}$ of 0.230 mmHg s mL⁻¹ (PVRI=8.39 Wood units·m²), in which a large additional stressed blood volume was required to increase the rotational frequency. One of the most important clinical questions is how systemic VAD augments cardiac output in high pulmonary vascular resistance. In our model, with a stepwise increase in PVRI, the cardiac index was maintained at more than 2.2 L/min/m², meaning no hypoperfusion in the Forrester's subset. On the other

hand, the central venous pressure remarkably increased with an increase in PVRI. If we define acceptable central venous pressure as less than 15 mmHg, systemic VAD tolerates PVRI less than 5 Wood units m^2 (Fig. 4). When the patients' PVRI is more than 5 Wood units m^2 , the use of sub-pulmonary VAD may be required.

Limitations

This study had several methodological limitations. First, the parameters used in the present model were fixed, except for a few parameters. A change in $R_{a,p}$ may affect other parameters, such as $C_{a,p}$ in the clinical setting. Further experimental and clinical implications are necessary to include interactions among the parameters in our simulation. Second, most patients with failing Fontan circulation have fenestrations or shunts, which were excluded in this model. These factors should affect the simulation results. In this study, we simplified the model to examine the effects of systemic VAD in patients with Fontan circulation. Because of the complexity of this circulation, it may be essential to simulate each patient using this method to understand the possible effects of systemic VAD. Third, venous systems have non-linearities, but non-linearities are omitted in the modified three-element Windkessel vasculature model. Because Mehlsen has reported that non-linearities in pressure/flow relationships need to be considered in low-flow conditions [30], the non-linearities of the venous systems may affect the simulation results, especially in the low-flow conditions of Fontan failure.

Conclusion

In the three models of Fontan failure (systolic ventricular, diastolic ventricular, or atrioventricular valve dysfunction), systemic VAD effectively increased the cardiac index and blood pressure. With an adequate reduction in the stressed blood volume, systemic VAD can decrease central venous pressure. In contrast, in Fontan failure with increased PVRI, central venous pressure increased even under systemic VAD support. Although further clinical investigations are needed, in patients with extremely high pulmonary vascular resistance of over 5 Wood units- m^2 , systemic VAD may be less effective, and sub-pulmonary VAD or biventricular VAD should be discussed.

Abbreviations

PVRI	Pulmonary vascular resistance index
SA	Single atrium
SV	Single ventricle
VAD	Ventricular assist device

Supplementary Information

The online version contains supplementary material available at <https://doi.org/10.1186/s12576-024-00946-z>.

Supplementary Material 1.

Acknowledgements

We would like to thank DeepL Write for English language editing.

Author contributions

EK, YK and SS conceived and designed the study. EK and SS performed the simulation. EK, YK, TS and SS analyzed data. EK, YK, TS, SK and SS interpreted the results of the simulation. EK, YK and SS prepared the figures and drafted the manuscript. EK, YK, TS, SK and SS edited and revised the manuscript. All authors read and approved the final manuscript.

Funding

This study was supported by the JSPS KAKENHI Grants Number JP19K09282, JP20K09266 and JP22K12794.

Availability of data and materials

The data sets used and analyzed during the current study and source codes are available from the corresponding author on reasonable request.

Declarations

Ethics approval and consent to participate

Not applicable.

Consent for publication

Not applicable.

Competing interests

The authors have no competing interests to declare.

Received: 14 June 2024 Accepted: 9 October 2024

Published online: 02 November 2024

References

- Fontan F, Baudet E (1971) Surgical repair of tricuspid atresia. *Thorax* 26:240–248
- d'Udekem Y, Iyengar AJ, Cochrane AD, Grigg LE, Ramsay JM, Wheaton GR et al (2007) The Fontan procedure: contemporary techniques have improved long-term outcomes. *Circulation* 116:1157–1164
- Rychik J, Atz AM, Celermajer DS, Deal BJ, Gatzoulis MA, Gewillig MH et al (2019) Evaluation and management of the child and adult with Fontan circulation: a scientific statement from the American Heart Association. *Circulation* 140:e234–284
- Sallmon H, Ovroutski S, Schleiger A, Photiadis J, Weber SC, Nordmeyer J et al (2021) Late Fontan failure in adult patients is predominantly associated with deteriorating ventricular function. *Int J Cardiol* 344:87–94
- King G, Ayer J, Celermajer D, Zentner D, Justo R, Disney P et al (2019) Atrioventricular valve failure in fontan palliation. *J Am Coll Cardiol* 73:810–822
- Prêtre R, Häussler A, Bettex D, Genoni M (2008) Right-sided univentricular cardiac assistance in a failing Fontan circulation. *Ann Thorac Surg* 86:1018–1020
- Moosmann J, Dittrich S, Purbojo A, Cesnjevar R (2020) RVAD implantation in a Fontan patient with protein-losing enteropathy as a bridge to transplant: Prêtre modification. *J Card Surg* 35:1721–1724
- Pekkan K, Frakes D, De Zelicourt D, Lucas CW, Parks WJ, Yoganathan AP (2005) Coupling pediatric ventricle assist devices to the Fontan circulation: simulations with a lumped-parameter model. *ASAIO J* 51:618–628

9. Di Molfetta A, Ferrari G, Iacobelli R, Filippelli S, Amodeo A (2017) Concurrent use of continuous and pulsatile flow ventricular assist device on a Fontan patient: a simulation study. *Artif Organs* 41:32–39
10. Di Molfetta A, Amodeo A, Fresiello L, Trivella MG, Iacobelli R, Pilati M et al (2015) Simulation of ventricular, cavo-pulmonary, and biventricular ventricular assist devices in failing Fontan. *Artif Organs* 39:550–558
11. Shimizu S, Shishido T, Une D, Kamiya A, Kawada T, Sano S et al (2010) Right ventricular stiffness constant as a predictor of postoperative hemodynamics in patients with hypoplastic right ventricle: a theoretical analysis. *J Physiol Sci* 60:205–212
12. Burkhoff D, Tyberg JV (1993) Why does pulmonary venous pressure rise after onset of LV dysfunction: a theoretical analysis. *Am J Physiol* 265:H1819–1828
13. Shimizu S, Une D, Shishido T, Kamiya A, Kawada T, Sano S et al (2011) Norwood procedure with non-valved right ventricle to pulmonary artery shunt improves ventricular energetics despite the presence of diastolic regurgitation: a theoretical analysis. *J Physiol Sci* 61:457–465
14. Shimizu S, Kawada T, Une D, Shishido T, Kamiya A, Sano S et al (2016) Hybrid stage I palliation for hypoplastic left heart syndrome has no advantage on ventricular energetics: a theoretical analysis. *Heart Vessels* 31:105–113
15. Morley D, Litwak K, Ferber P, Spence P, Dowling R, Meyns B et al (2007) Hemodynamic effects of partial ventricular support in chronic heart failure: results of simulation validated with in vivo data. *J Thorac Cardiovasc Surg* 133:21–28
16. Girfoglio M, Ballarin F, Infantino G, Nicoló F, Montalto A, Rozza G et al (2022) Non-invasive PODI-ROM for patient-specific aortic blood flow in presence of a LVAD device. *Med Eng Phys* 107:103849
17. Egbe AC, Connolly HM, Miranda WR, Ammash NM, Hagler DJ, Veldtman GR et al (2017) Hemodynamics of Fontan failure: the role of pulmonary vascular disease. *Circ Heart Fail* 10:e004515
18. Fahnhorst SE, Brandewie K, Perry T, Opotowsky AR, Lubert AM, Lorts A et al (2023) Single center experience with durable continuous flow single ventricle assist device: a viable option in fontan circulatory failure. *ASAIO J* 69:956–961
19. Anderson PA, Sleeper LA, Mahony L, Colan SD, Atz AM, Breitbart RE et al (2008) Contemporary outcomes after the Fontan procedure: a Pediatric Heart Network multicenter study. *J Am Coll Cardiol* 52:85–98
20. Atz AM, Zak V, Mahony L, Uzark K, D'agincourt N, Goldberg DJ et al (2017) Longitudinal outcomes of patients with single ventricle after the Fontan procedure. *J Am Coll Cardiol* 69:2735–2744
21. Kotani Y, Chetan D, Zhu J, Saedi A, Zhao L, Mertens L et al (2018) Fontan failure and death in contemporary Fontan circulation: analysis from the last two decades. *Ann Thorac Surg* 105:1240–1247
22. Milanese O, Stellin G, Colan SD, Facchin P, Crepaz R, Biffanti R et al (2002) Systolic and diastolic performance late after the Fontan procedure for a single ventricle and comparison of those undergoing operation at <12 months of age and at >12 months of age. *Am J Cardiol* 89:276–280
23. Garofalo CA, Cabreriza SE, Quinn TA, Weinberg AD, Printz BF, Hsu DT et al (2006) Ventricular diastolic stiffness predicts perioperative morbidity and duration of pleural effusions after the Fontan operation. *Circulation* 114:156–61
24. King G, Buratto E, Celermajer DS, Grigg L, Alphonso N, Robertson T et al (2022) Natural and modified history of atrioventricular valve regurgitation in patients with Fontan circulation. *J Am Coll Cardiol* 79:1832–1845
25. King G, Gentles TL, Winlaw DS, Cordina R, Bullock A, Grigg LE et al (2017) Common atrioventricular valve failure during single ventricle palliation. *Eur J Cardiothorac Surg* 51:1037–1043
26. Sugimoto K, Konstantinov IE, Brizard CP, d'Udekem Y (2015) Polytetrafluoroethylene bridge for atrioventricular valve repair in single-ventricle palliation. *J Thorac Cardiovasc Surg* 149:641–643
27. Ando M, Takahashi Y (2007) Edge-to-edge repair of common atrioventricular or tricuspid valve in patients with functionally single ventricle. *Ann Thorac Surg* 84:1571–1576
28. Cedars A, Kutty S, Danford D, Schumacher K, Learning Network Investigators ACTION (2021) Systemic ventricular assist device support in Fontan patients: a report by ACTION. *J Heart Lung Transplant* 40:368–376
29. Nandi D, Miller KD, Bober CM, Rosenthal TM, Montenegro LM, Rossano JW et al (2018) Systemic atrioventricular valve excision and ventricular assist devices in pediatric patients. *Ann Thorac Surg* 105:170–174
30. Mehlsen J (2000) Models of the venous system. *Stud Health Technol Inform* 71:109–117

Publisher's Note

Springer Nature remains neutral with regard to jurisdictional claims in published maps and institutional affiliations.